

# Analysis of the HELIOS-3 $\mu^+\mu^-$ Data within a Relativistic Transport Approach\*

W. Cassing<sup>1</sup>, W. Ehehalt<sup>1</sup> and I. Kralik<sup>2</sup>

<sup>1</sup> Institut für Theoretische Physik, Universität Giessen  
D-35392 Giessen, Germany

<sup>2</sup> Institute of Experimental Physics, Slovak Academy of Sciences  
SR-04353 Kosice

April 16, 2018

## Abstract

We present a nonperturbative dynamical study of  $\mu^+\mu^-$  production in proton-nucleus and nucleus-nucleus collisions at SPS energies on the basis of the covariant transport approach HSD. For p + W reactions at 200 GeV bombarding energy the dimuon yield for invariant masses  $m \leq 1.6$  GeV is found to be dominated by the decays of the  $\eta, \rho, \omega$  and  $\Phi$  mesons. For 200 GeV/A S + W collisions, however, the dimuon yield shows an additional large contribution from  $\pi^+\pi^-$ ,  $K^+K^-$  and  $\pi\rho$  channels. We find that for ‘free’ meson masses and form factors the experimental cross section is clearly underestimated for S + W in the invariant mass range  $0.35 \text{ GeV} \leq m \leq 0.65 \text{ GeV}$  and that the HELIOS-3 data can only be reproduced within a hadronic scenario, if the  $\rho/\omega$ -meson mass drops with baryon density. This finding suggests a partial restoration of chiral symmetry in S + W collisions at SPS energies.

PACS: 25.75+r 14.60.-z 14.60.Cd

Keywords: relativistic heavy-ion collisions, leptons

---

\*Work supported by BMBF and GSI Darmstadt.

The question of chiral symmetry restoration at high baryon density is of fundamental interest since a couple of years [1, 2], but a clear experimental evidence has not been achieved, so far. The enhancement of strangeness production as e.g. seen in the AGS data for the  $K^+/\pi^+$  ratio [3] might be a signature for such a transition [4], however, other hadronic scenarios can be cooked up to describe this phenomenon as well [5]. On the other hand, dileptons are particularly well suited for an investigation of the violent phases of a high-energy heavy-ion collision because they can leave the reaction volume essentially undistorted by final-state interactions. Indeed, dileptons from heavy-ion collisions have been observed by the DLS collaboration at the BEVALAC [6, 7, 8] and by the CERES [9] and HELIOS collaboration [10, 11] at SPS energies.

The enhancement of the low mass dimuon yield in S + W compared to p + W collisions [10] has been first suggested by Koch et al. [12] to be due to  $\pi^+\pi^-$  annihilation. Furthermore, Li et al. [13] have proposed that the enhancement of the  $e^+e^-$  yield in S + Au collision as observed by the CERES collaboration [9] should be due to an enhanced  $\rho$ -meson production (via  $\pi^+\pi^-$  annihilation) and a dropping  $\rho$ -mass in the medium. In fact, their analysis - which was based on an expanding fireball scenario in chemical equilibrium - could be confirmed within the microscopic transport calculations in ref. [14]; however, also a more conventional approach including the increase of the  $\rho$ -meson width in the medium due to the coupling of the  $\rho, \pi, \Delta$  and nucleon dynamics [15, 16, 17] was found to be compatible with the CERES data. In this paper, we will carry out a similar study as in ref. [14] but for the dimuon data of the HELIOS-3 collaboration [10] which provide independent information on dilepton production with rather good statistics.

In continuation of the dilepton production studies in refs. [14, 18, 19, 20] we describe the dynamics of proton-nucleus or nucleus-nucleus reactions by a coupled set of covariant transport equations with scalar and vector self-energies of all hadrons involved. Explicitly propagated are nucleons,  $\Delta$ 's,  $N^*(1440)$ ,  $N^*(1535)$  resonances as well as  $\pi$ 's,  $\eta$ 's,  $\rho$ 's,  $\omega$ 's,  $\Phi$ 's, kaons and  $K^*$ 's with their isospin degrees of freedom. For more detailed information on the self-energies employed we refer the reader to ref. [4], where the transport approach HSD<sup>1</sup> is formulated and applied to nucleus-nucleus collisions from SIS to SPS energies.

In this analysis we calculate  $\mu^+\mu^-$  production taking into account the contributions from nucleon-nucleon, pion-nucleon and pion-pion bremsstrahlung, the Dalitz-decays  $\eta \rightarrow \gamma\mu^+\mu^-$  and  $\omega \rightarrow \pi^0\mu^+\mu^-$ , the direct dimuon decays of the vector mesons  $\rho, \omega, \Phi$  as well as  $\pi^+\pi^-$ ,  $K^+K^-$  and  $\pi\rho$  production channels. The nucleon-nucleon, pion-nucleon and  $\pi\pi$

---

<sup>1</sup>Hadron-String-Dynamics

bremsstrahlung are evaluated in a phase-space corrected soft photon approximation as described in refs. [18, 20]. Though this limit is questionable for the bombarding energy of interest, the soft photon approximation provides an upper limit for the bremsstrahlung contribution [21], which will turn out to be small in comparison to the meson decay channels.

The pion annihilation proceeds through the  $\rho$ -meson which decays into a virtual massive photon by vector meson dominance. The cross section is parametrized as [18, 20, 22]

$$\sigma^{\pi^+\pi^-\rightarrow\mu^+\mu^-}(m) = \frac{4\pi}{3} \left(\frac{\alpha}{m}\right)^2 \sqrt{1 - \frac{4m_\pi^2}{m^2}} |F_\pi(m)|^2, \quad (1)$$

where the free form factor of the pion is approximated by

$$|F_\pi(m)|^2 = \frac{m_\rho^4}{(m^2 - m_\rho^2)^2 + m_\rho^2 \Gamma_\rho^2}. \quad (2)$$

In eq. (2)  $m$  is the dilepton invariant mass,  $\alpha$  is the fine structure constant, and

$$m_\rho = 775 \text{ MeV}, \quad \Gamma_\rho = 118 \text{ MeV}.$$

So far, eq.(1) describes the free pion annihilation cross section; possible medium modifications of the  $\rho$ -meson will be discussed below.

The cross section for the  $K^+K^-$  annihilation is parametrized as [23]

$$\sigma^{K^+K^-\rightarrow\mu^+\mu^-}(m) = \frac{4\pi}{3} \left(\frac{\alpha}{m}\right)^2 \sqrt{1 - \frac{4m_K^2}{m^2}} |F_K(m)|^2, \quad (3)$$

where the free form factor of the kaon is approximated by

$$|F_K(m)|^2 = \frac{1}{9} \frac{m_\Phi^4}{(m^2 - m_\Phi^2)^2 + m_\Phi^2 \Gamma_\Phi^2} \quad (4)$$

with

$$m_\Phi = 1020 \text{ MeV}, \quad \Gamma_\Phi = 4.43 \text{ MeV}.$$

The cross section for dimuon production in  $\pi^+\rho^-$ ,  $\pi^-\rho^+$  scattering is given by the Breit-Wigner cross section [24] for the formation of a  $\Phi$ -meson times the partial decay of the  $\Phi$  into a  $\mu^+\mu^-$  pair,

$$\sigma^{\pi^+\rho^-\rightarrow\mu^+\mu^-}(m) = \frac{\pi}{k^2} \frac{\Gamma_t^2}{(m - m_\Phi)^2 + \Gamma_t^2/4} B_{in} B_{out},$$

$$\Gamma_t(k) = \Gamma_\Phi \left(\frac{k}{k_r}\right)^3 \frac{k_r^2 + q^2}{k^2 + q^2},$$

$$\begin{aligned}
q^2 &= (m_\Phi - m_\rho - m_\pi)^2 + \Gamma_\Phi^2/4, \\
k_r^2 &= (m_\Phi^2 - (m_\rho + m_\pi)^2) (m_\Phi^2 - (m_\rho - m_\pi)^2) / (4m_\Phi^2), \\
k^2 &= (m^2 - (m_\rho + m_\pi)^2) (m^2 - (m_\rho - m_\pi)^2) / (4m^2),
\end{aligned} \tag{5}$$

with  $B_{in} = 0.13$  and  $B_{out} = 2.5 \times 10^{-4}$ . We note that the resonance approximation (5) also works very well for  $K^+K^-$  annihilation as described by eq. (3) when including a further spin factor of 3 and  $B_{in} = 0.49$ .

The  $\omega$  Dalitz-decay, furthermore, is given by [25]:

$$\begin{aligned}
\frac{d\Gamma_{\omega \rightarrow \pi^0 \mu^+ \mu^-}}{dm} &= \frac{\alpha}{3\pi} \frac{\Gamma_{\omega \rightarrow \pi^0 \gamma}}{m} \left(1 - \frac{4m_\mu^2}{m^2}\right)^{1/2} \left(1 + 2\frac{m_\mu^2}{m^2}\right) \\
&\times \left( \left(1 + \frac{m^2}{m_\omega^2 - m_\pi^2}\right)^2 - \frac{4m_\omega^2 m^2}{(m_\omega^2 - m_\pi^2)^2} \right)^{3/2} |F_{\omega \rightarrow \pi^0 \mu^+ \mu^-}(m)|^2,
\end{aligned} \tag{6}$$

where the form factor is parametrized as

$$F_{\omega \rightarrow \pi^0 \mu^+ \mu^-}(m) = \frac{\Lambda_s^4}{(\Lambda_s^2 - m^2)^2 + \Lambda_s^2 \Gamma_s^2} \tag{7}$$

with

$$\Lambda_s = 0.60 \text{ GeV}, \quad \Gamma_s = 75 \text{ MeV}. \tag{8}$$

The form (7) for  $F_\omega$  is actually fitted to the dimuon data for  $p + W$  at 200 GeV for  $0.4 \text{ GeV} \leq m \leq 0.6 \text{ GeV}$  and slightly deviates from the parametrization in [25] (with  $\Lambda_s = 0.65 \pm 0.03 \text{ GeV}$ ) but is still compatible with the data presented in [25]. We note that this formfactor is of interest in its own since it shows a significant enhancement compared to the vector-meson-dominance model [25]. More accurate experimental data on this formfactor as well as further theoretical studies will be needed to clarify the underlying physics.

The direct decays of the vector mesons to  $\mu^+ \mu^-$  are taken as

$$\frac{d\sigma}{dm^2}(m) = \frac{1}{\pi} \frac{m_V \Gamma_V}{(m^2 - m_V^2)^2 + m_V^2 \Gamma_V^2} \frac{\Gamma_{V \rightarrow \mu^+ \mu^-}}{\Gamma_{tot}} \tag{9}$$

with  $\Gamma_{\Phi \rightarrow \mu^+ \mu^-} / \Gamma_\Phi^{tot} = 2.5 \times 10^{-4}$ ,  $\Gamma_{\omega \rightarrow \mu^+ \mu^-} / \Gamma_\omega^{tot} = 7.1 \times 10^{-5}$  and  $\Gamma_{\rho \rightarrow \mu^+ \mu^-} / \Gamma_\rho^{tot} = 4.6 \times 10^{-5}$ . Though of minor importance we also include the direct decay of the  $\eta$ -meson with  $\Gamma_{\eta \rightarrow \mu^+ \mu^-} / \Gamma_\eta^{tot} = 5.7 \times 10^{-6}$ . The charged particle multiplicity  $N_c$  - which also provides the normalization of the experimental data - is recorded in the pseudorapidity interval  $3.7 \leq \eta \leq 5.2$ .

Transport models similar to ours have been applied for  $e^+e^-$  production at BEVALAC energies in refs. [26, 27, 28, 29] and at AGS energies in [30]. The first full microscopic

studies for  $e^+e^-$  production at SPS energies have been reported in [14]; the same covariant transport approach is also used in our present analysis.

We have calculated the  $\mu^+\mu^-$  yield for p + W at 200 GeV using the experimental cuts in rapidity  $y$  and transverse mass  $m_T$  of the dimuon source,

$$m_T \geq 4(7 - 2y), \quad m_T \geq \sqrt{(2m_\mu)^2 + \left(\frac{15 \text{ GeV}/c}{\cosh(y)}\right)^2}, \quad (10)$$

as well as the experimental resolution in energy [10].

Our results are displayed in Fig. 1 for p + W at 200 GeV in comparison with the HELIOS-3 data [10]. In the upper part of Fig. 1 we show the calculated results with an energy resolution of  $\Delta_M = 15$  MeV, while the experimental resolution was used in the lower part of Fig. 1 in order to demonstrate the sensitivity of the spectra to the actual mass resolution in the experimental data. The full solid curves in Fig. 1 display the sum of all individual contributions which is dominated by the decays of the mesons. The bremsstrahlung contributions ( $\pi$ N, pN and  $\pi\pi$  channels summed up in the single line denoted by 'brems') as well as  $\pi^+\pi^-$  annihilation (short dashed line) are of minor importance for the proton induced reaction in full analogy to the CERES  $e^+e^-$  data [9, 14]. The very good reproduction of the HELIOS-3 data, where medium effects are negligible, allows us to perform a related analysis of nucleus-nucleus collisions with particular emphasis on medium properties of the reaction channels involved.

We thus go over to the system S + W at 200 GeV/A where we expect to describe the global reaction dynamics with the same quality as for S + Au at 200 GeV/A (cf. Fig. 2 of [14]). The results of our calculation, where no medium effects are incorporated for all mesons, are displayed in Fig. 2 (thick solid line) in comparison to the data [10]. The individual contributions from bremsstrahlung channels (denoted by 'brems'),  $\eta$  and  $\omega$  Dalitz decays as well as direct vector meson decays are explicitly indicated in Fig. 2. Concentrating on the invariant mass range  $m \leq 1$  GeV we find the experimental yield to be underestimated for  $0.35 \text{ GeV} \leq m \leq 0.65 \text{ GeV}$  and slightly overestimated for  $m \approx 0.8 \text{ GeV}$ . In the  $\Phi$ -mass region the cross section includes the direct  $\Phi$  production channels as well as those from  $\pi\rho$  and  $K^+K^-$  collisions<sup>2</sup>. The  $\pi^+\pi^-$  annihilation component (short dashed line) is found to be of the same order of magnitude as the direct  $\rho$ -decay (long dashed line) within the experimental cuts and significantly smaller than in case of the CERES data [14] - which focus on the mid-rapidity regime - while the additional bremsstrahlung contributions again are of minor importance.

---

<sup>2</sup>The kaon production channels  $\pi\pi \rightarrow K\bar{K}$  are included in the transport calculation

Since the reproduction of the HELIOS-3 data in Fig. 2 is rather poor we will now explore possible in-medium modifications of the mesons as advocated in refs. [14, 20, 23, 26, 31]. Before going over to the actual model, we show in Fig. 3 for S + W at 200 GeV/A the  $\rho$ -mass distribution versus the baryon density  $\rho_B$  in units of  $\rho_0 \approx 0.168 fm^{-3}$ , where the baryon density is computed in the local rest frame, i.e.  $\rho_B^2(x) = j_\mu j^\mu$ , while  $j_\mu(x)$  denotes the Lorentz invariant baryon current. In Fig. 3 the solid line represents the distribution of  $\rho$ 's produced in baryon-baryon and pion-baryon collisions whereas the dashed line corresponds to those from  $\pi^+\pi^-$  annihilation. We note that the distributions in Fig. 3 are recorded at the creation time of the  $\rho$ -mesons, whereas the distribution at the actual decay time is slightly shifted to smaller density. Furthermore, only those  $\rho$ -mesons have been considered which fulfill the experimental cuts (10) in order to provide a close connection to the HELIOS-3 experiment. These distributions clearly indicate that most of the  $\rho$ 's are produced at nonzero baryon density and even for  $\rho_B \geq 3\rho_0$ .

We now turn to the possible modifications of the  $\rho$ -meson in the medium. From QCD inspired models [1, 31] or estimates based on QCD sum rules [32, 33] it has been predicted that the  $\rho$ -meson mass decreases with density. In order to explore the compatibility of such scenarios with the HELIOS-3 data, we have performed calculations with a medium-dependent  $\rho$ - (and  $\omega$ )-mass according to Hatsuda and Lee [32], i.e.

$$m_\rho^* \approx m_\rho^0 (1 - 0.18\rho_B/\rho_0) \geq m_u + m_d \approx 14MeV, \quad (11)$$

where  $\rho_B(t)$  is the actual baryon density during the decay of the  $\rho$ -meson. A similar scaling with density has also been predicted by Shakin et al. [31]. Since the width of the  $\rho$ -meson is determined by the decay into two pions, which are propagated without selfenergies as in [4], we have parametrized the in-medium width  $\Gamma_\rho^*$  as

$$\Gamma_\rho^* = \Gamma_\rho \frac{m_\rho^{*2} - 4m_\pi^2}{m_\rho^2 - 4m_\pi^2} \Theta(m_\rho^* - 2m_\pi). \quad (12)$$

The dropping of the  $\rho$ -meson mass is associated with a scalar self-energy of the meson which is determined by the local baryon density; the propagation of the 'quasi-particle' with effective mass  $m_\rho^*$  thus couples to the baryon current during the expansion, and the meson becomes 'on-shell' asymptotically due to a feedback of energy from the mean fields, which thus ensures that the total energy of the system is conserved.

The results of this simulation are shown in Fig. 4 in comparison with the HELIOS-3 data. The  $\pi^+\pi^-$  annihilation component (short dashed line) now shows a peak at invariant masses  $m \approx 0.6$  GeV and leads to a significant enhancement of low mass dileptons. A

further enhancement at lower masses is also provided by the direct  $\rho$ -decays (long dashed line) due to their shifted masses. In comparison to Fig. 2 the experimental dimuon spectrum is now much better reproduced for invariant masses  $m \leq 1$  GeV; the missing yield for  $m \geq 1.2$  GeV might be due to direct charm production channels or higher meson resonances which are not explicitly included in the present calculations.

Of further interest is the experimental rapidity dependence of the dimuon spectra. Here, explicit data are available within the cuts (10) for  $y \leq 3.9$ ,  $3.9 \leq y \leq 4.4$ , and  $y \geq 4.4$ . The comparison of our calculations with the data is shown in Fig. 5 for the rapidity cuts  $3.9 \leq y \leq 4.4$  and  $y \geq 4.4$ . The dotted lines correspond to calculations with free meson masses and formfactors whereas the solid lines are the result within the dropping meson mass scenario (11) with the in-medium width (12). Again the computations with free meson masses fail to reproduce the data especially for the lower rapidity interval from 0.35 - 0.65 GeV and about 0.8 GeV whereas the agreement is remarkably fine when including the shift of the meson masses with density.

As advocated by Haglin [34] the width of the  $\rho$ -meson should again increase in a dense mesonic environment due to the mesonic interaction channels. In order to explore such effects we have performed calculations with a dropping  $\rho$ -mass according to (11), however, keeping its width at the free value, i.e.  $\Gamma_\rho^* = \Gamma_\rho$ . The results of this 'theoretical experiment' are displayed in Fig. 5 in terms of the dashed lines. Whereas for  $y \geq 4.4$  the agreement with the data improves, the  $\mu^+\mu^-$  yield is slightly underestimated for  $m \approx 0.5$  GeV in the lower rapidity interval. We thus cannot extract a clear evidence for a reduced width of the  $\rho$ -meson at high baryon density from the present experimental data.

Within the same spirit we have also investigated, if the broadening of the  $\rho$ -meson - without a shift of its pole - according to Herrmann et al. [15], which is due to the coupled  $\pi$  and  $\Delta$ -hole dynamics, might improve the description of the data. However, contrary to the  $e^+e^-$  spectra of the CERES-collaboration (cf. ref. [14]), there is no significant enhancement of the spectra for  $0.3 \text{ GeV} \leq m \leq 0.6 \text{ GeV}$  (in comparison to Fig. 2) such that this mechanism can no longer be considered as dominant. Furthermore, since the pion densities in the rapidity regime of interest are large compared to the baryon densities (cf. Fig. 2 of [14]), the pion selfenergy effects from  $\Delta$ -hole loops are most likely overestimated [35].

In summary, we have studied  $\mu^+\mu^-$  production in proton and heavy-ion induced reactions at 200 GeV/A on the basis of the covariant transport approach HSD [4]. We have incorporated the contributions from proton-nucleon, pion-nucleon and pion-pion bremsstrahlung, the Dalitz-decay of the  $\Delta$ ,  $\eta$  and  $\omega$  as well as  $\pi^+\pi^-$  annihilation and the

direct dilepton decay of the vector mesons  $\rho, \omega, \Phi$  as well as  $K^+K^-$  and  $\pi\rho$  channels. It is found that for  $p + W$  at 200 GeV the mesonic decays almost completely determine the dilepton yield, whereas in  $S + W$  reactions the  $\pi^+\pi^-, K^+K^-$  annihilation channels and  $\pi\rho$  collisions contribute substantially. The experimental data taken by the HELIOS-3 collaboration [10] are underestimated by the calculations for invariant masses  $0.35 \text{ GeV} \leq m \leq 0.65 \text{ GeV}$  when using free form factors for the pion and  $\rho$ -meson.

We have, furthermore, examined if a shift of the  $\rho$ - (and  $\omega$ )-mass according to QCD sum rules - as suggested by Hatsuda and Lee [32] or Shakin et al. [31] - is compatible with the data as in case of the  $e^+e^-$  spectra of the CERES collaboration [14]. Indeed the description of the  $\mu^+\mu^-$  spectrum improves substantially within this 'dropping mass' scenario at all rapidity bins. However, the effects at forward rapidities are not as pronounced as close to midrapidity where the dilepton yield is clearly dominated by the  $\pi^+\pi^-$  annihilation channel (cf. Figs. 3-5 of [14]). Nevertheless, the explicit rapidity dependence of the experimental dimuon spectra, which is in line with the dropping meson mass scenario, provides a strong hint for the partial restoration of chiral symmetry at high baryon density. Data with high statistics especially at midrapidity or alternatively central collisions of  $Pb + Pb$  at SPS-energies are expected to allow for more definite conclusions about the chiral phase transition of hadronic matter at  $4-6 \times \rho_0$  baryon density.

The authors gratefully acknowledge many helpful discussions with E. L. Bratkovskaya, K. Haglin, C. M. Ko, U. Mosel, H. J. Specht, and Gy. Wolf. They are especially indebted to A. Drees for many hints and fruitful suggestions throughout the course of this analysis.

## References

- [1] G. Brown and M. Rho, Phys. Rev. Lett. 66 (1991) 2720.
- [2] M. C. Birse, J. Phys. G20 (1994) 1537.
- [3] T. Abbot *et al.*, Nucl. Phys. A544 (1992) 237.
- [4] W. Ehehalt and W. Cassing, Nucl. Phys. A, submitted; hep-ph/9507274.
- [5] B. Braun-Munzinger, J. Stachel, J. P. Wessels, and N. Xu, Phys. Lett. B344 (1995) 43.
- [6] G. Roche *et al.*, Phys. Rev. Lett. 61 (1988) 1069.



- [7] C. Naudet *et al.*, Phys. Rev. Lett. 62 (1989) 2652.
- [8] G. Roche *et al.*, Phys. Lett. B226 (1989) 228.
- [9] G. Agakichiev *et al.*, Phys. Rev. Lett. 75 (1995) 1272; A. Drees, Proceedings of the 'International Symposium on Multiparticle Dynamics', Stara Lesna, Sep. 1995.
- [10] M. A. Mazzoni, Nucl. Phys. A566 (1994) 95c; M. Masera, Nucl. Phys. A590 (1995) 93c; I. Kralik and the HELIOS-3 collaboration, Proceedings of the International Workshop XXIII on Gross Properties of Nuclei and Nuclear Excitations, Hirschegg, Austria, Jan. 1995, ed. by H. Feldmeier and W. Nörenberg, p. 143.
- [11] T. Akesson *et al.*, Z. Phys. C68 (1995) 47.
- [12] P. Koch, Phys. Lett. B288 (1992) 187; B. Kämpfer, P. Koch, and O. P. Pavlenko, Phys. Rev. C49 (1994) 1132.
- [13] G. Q. Li, C. M. Ko, and G. E. Brown, Phys. Rev. Lett. 75 (1995) 4007.
- [14] W. Cassing, W. Ehehalt, and C. M. Ko, Phys. Lett. B363 (1995) 35.
- [15] M. Herrmann, B. Friman, and W. Nörenberg, Nucl. Phys. A560 (1993) 411.
- [16] M. Asakawa, C. M. Ko, P. Lévai, and X. J. Qiu, Phys. Rev. C46 (1992) R1159.
- [17] G. Chanfray and P. Schuck, Nucl. Phys. A545 (1992) 271c.
- [18] Gy. Wolf, G. Batko, W. Cassing *et al.*, Nucl. Phys. A517 (1990) 615.
- [19] Gy. Wolf, W. Cassing, U. Mosel, and M. Schäfer, Phys. Rev. C43 (1991) R1501.
- [20] Gy. Wolf, W. Cassing, and U. Mosel, Nucl. Phys. A552 (1993) 549.
- [21] H. Eggers, private communication.
- [22] C. Gale and J. Kapusta, Phys. Rev., C35 (1987) 2107.
- [23] G. Q. Li and C. M. Ko, Nucl. Phys. A582 (1995) 731.
- [24] W. Cassing, V. Metag, U. Mosel, and K. Niita, Phys. Rep. 188 (1990) 363.
- [25] L. G. Landsberg, Phys. Rep. 128 (1985) 301.
- [26] L.H. Xia, C.M. Ko, L. Xiong, and J.Q. Wu, Nucl. Phys. A485 (1988) 721.

- [27] L. Xiong, Z.G. Wu, C.M. Ko, and J.Q. Wu, Nucl. Phys. A512 (1990) 772.
- [28] V.D. Toneev, A.I. Titov, and K.K. Gudima, GSI-92-05 preprint (1992).
- [29] V. D. Toneev, E. L. Bratkovskaya, and K. K. Gudima, Proceedings of the International Workshop XXIII on Gross Properties of Nuclei and Nuclear Excitations, Hirschegg, Austria, Jan. 1995, ed. by H. Feldmeier and W. Nörenberg, p. 330.
- [30] L. A. Winckelmann, H. Stöcker, W. Greiner, and H. Sorge, Phys. Lett. B298 (1993) 22; Phys. Rev. C51 (1995) R9.
- [31] C. M. Shakin and Wei-Dong Sun, Phys. Rev. C49 (1994) 1185.
- [32] T. Hatsuda and S. Lee, Phys. Rev. C46 (1992) R34.
- [33] M. Asakawa and C. M. Ko, Phys. Rev. C48 (1993) R526; Nucl. Phys. A560 (1993) 399.
- [34] K. Haglin, Nucl. Phys. A584 (1995) 719.
- [35] G. E. Brown, private communication.

## Figure Captions

**Fig. 1:** Comparison of our calculations for the differential dimuon spectra (thick solid line) with the experimental data [10] for p + W at 200 GeV. Upper part: with an energy resolution of 15 MeV; lower part: with the experimental resolution. The individual contributions from the vector mesons and Dalitz decays as well as bremsstrahlung channels are directly indicated in the figure. The  $\pi^+\pi^-$  annihilation channel and the decay from  $\rho$ -mesons produced in baryon-baryon and meson-baryon collisions are shown by the short dashed and long dashed lines, respectively.

**Fig. 2:** Comparison of our calculations for the differential dimuon spectra (upper thick solid line) with the experimental data [10] for S + W at 200 GeV/A when employing no

medium modification of the mesons. The  $\pi^+\pi^-$  annihilation channel and the decay from  $\rho$ -mesons produced in baryon-baryon and meson-baryon collisions are shown by the short dashed and long dashed lines, respectively.

**Fig. 3:** The  $\rho$ -mass distribution as a function of the baryon density  $\rho_B$  (in units of  $\rho_0$ ) for a central S + W reaction at 200 GeV/A within the HELIOS-3 acceptance (10). Solid line:  $\rho$ -mesons from baryon-baryon and meson-baryon reaction channels; dashed line:  $\rho$ -mesons from  $\pi^+\pi^-$  annihilation.

**Fig. 4:** Comparison of our calculations for the differential dimuon spectra (thick solid line) with the experimental data [10] for S + W at 200 GeV/A when including a shift of the  $\rho$ -meson mass (11) according to the prediction by Hatsuda and Lee [32] and a decrease of its width according to (12). The  $\pi^+\pi^-$  annihilation channel and the decay from  $\rho$ -mesons produced in baryon-baryon and meson-baryon collisions are shown by the short dashed and long dashed lines, respectively.

**Fig. 5:** Result of our calculations for the differential dimuon spectra for the rapidity cuts  $3.9 \leq y \leq 4.4$  and  $y \geq 4.4$  for S + W at 200 GeV/A in comparison to the HELIOS-3 data [10]. The dotted lines correspond to a calculation with free meson masses and formfactors, the solid lines to a calculation with a dropping  $\rho$ -mass according to (11) and width (12), whereas the dashed line is obtained in the dropping  $\rho$ -mass scenario (11) with the free  $\rho$ -meson width.

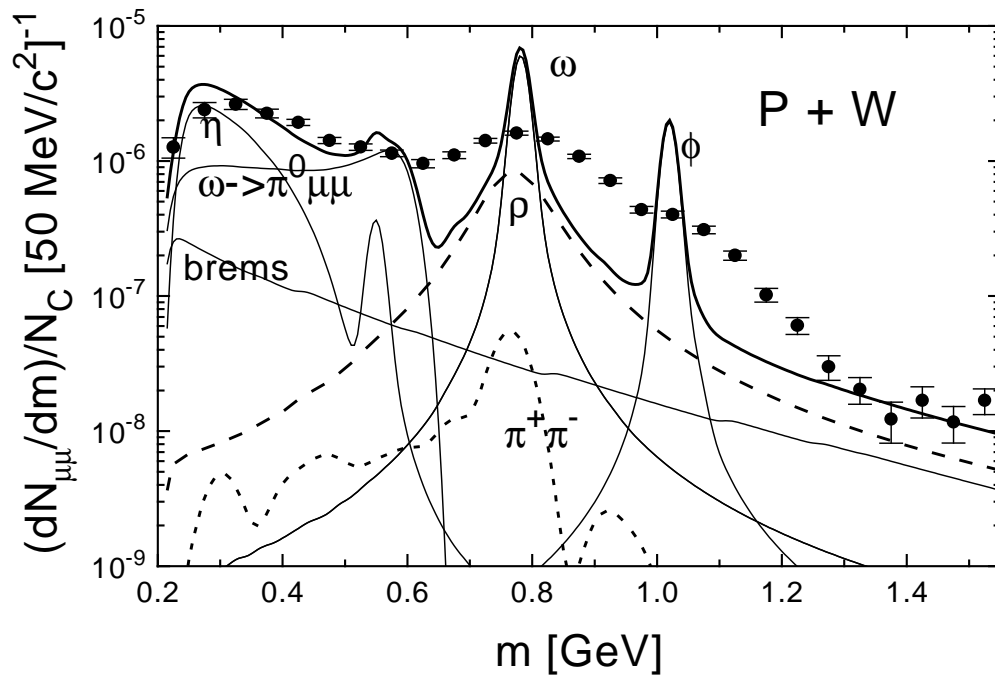


Figure 1a

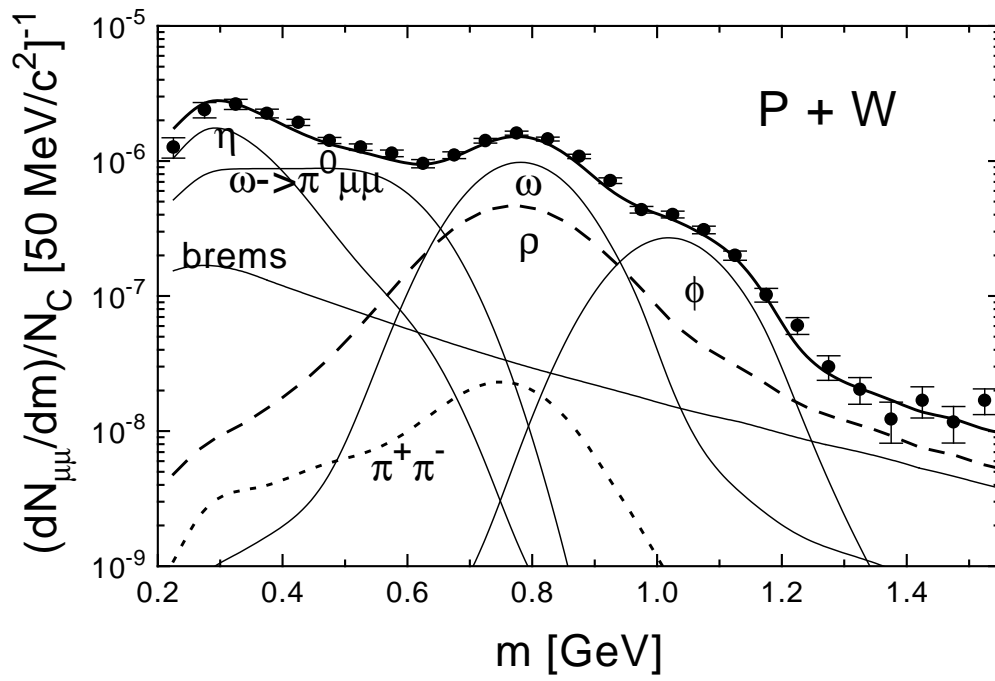


Figure 1b

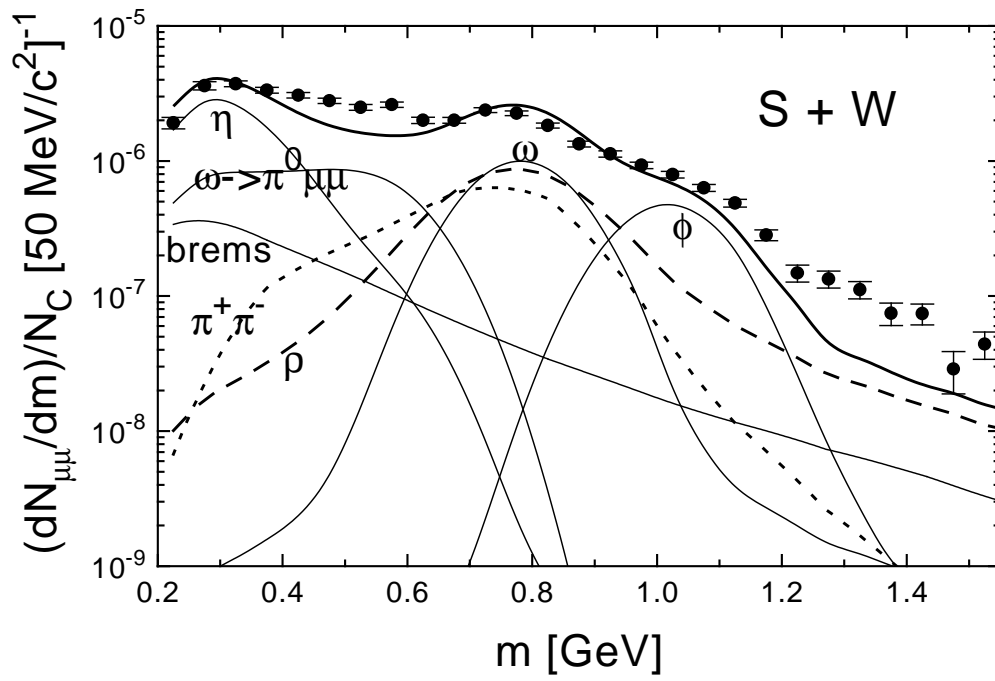


Figure 2

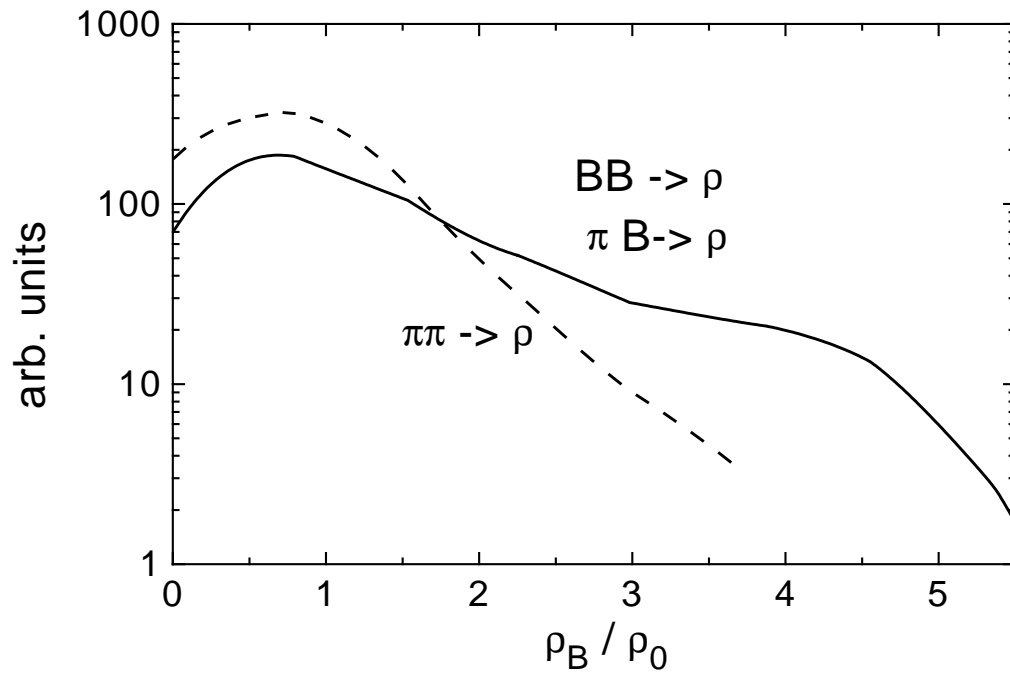


Figure 3

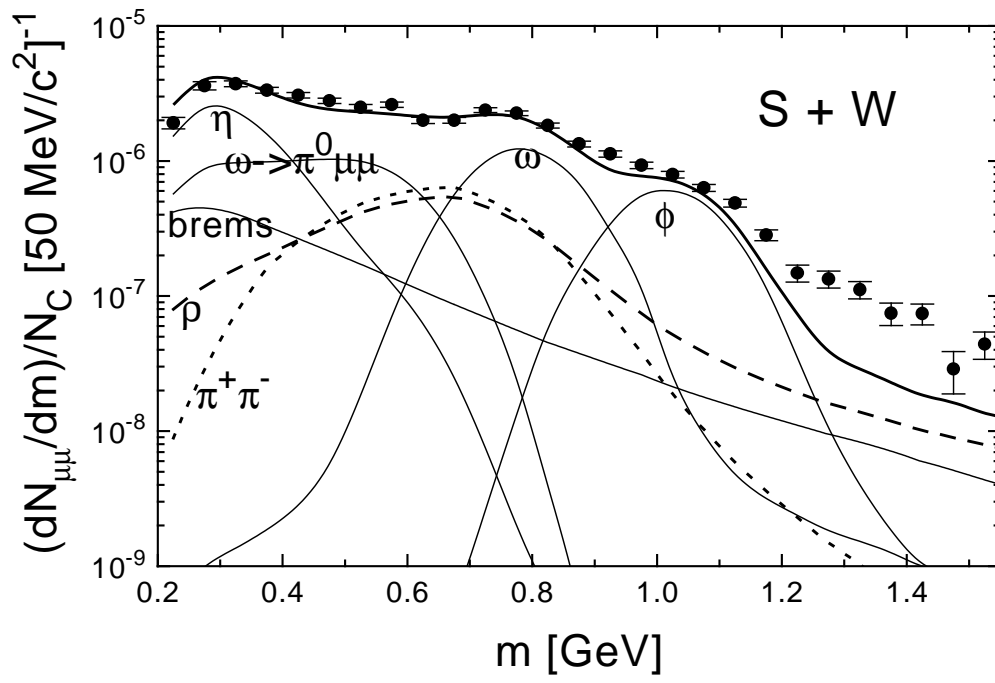


Figure 4



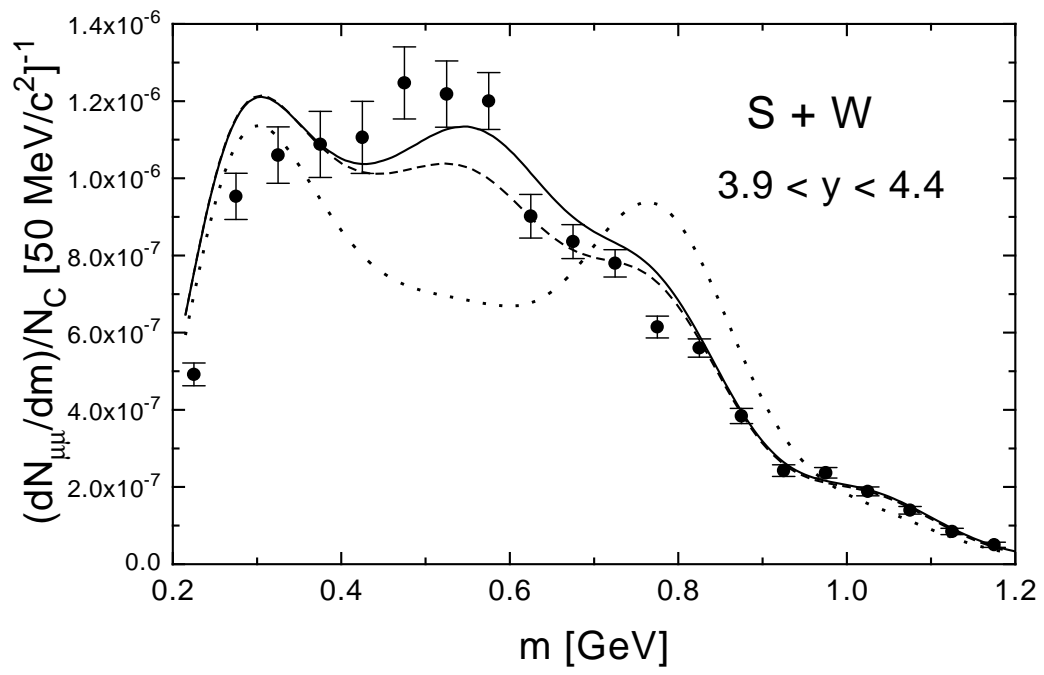


Figure 5a

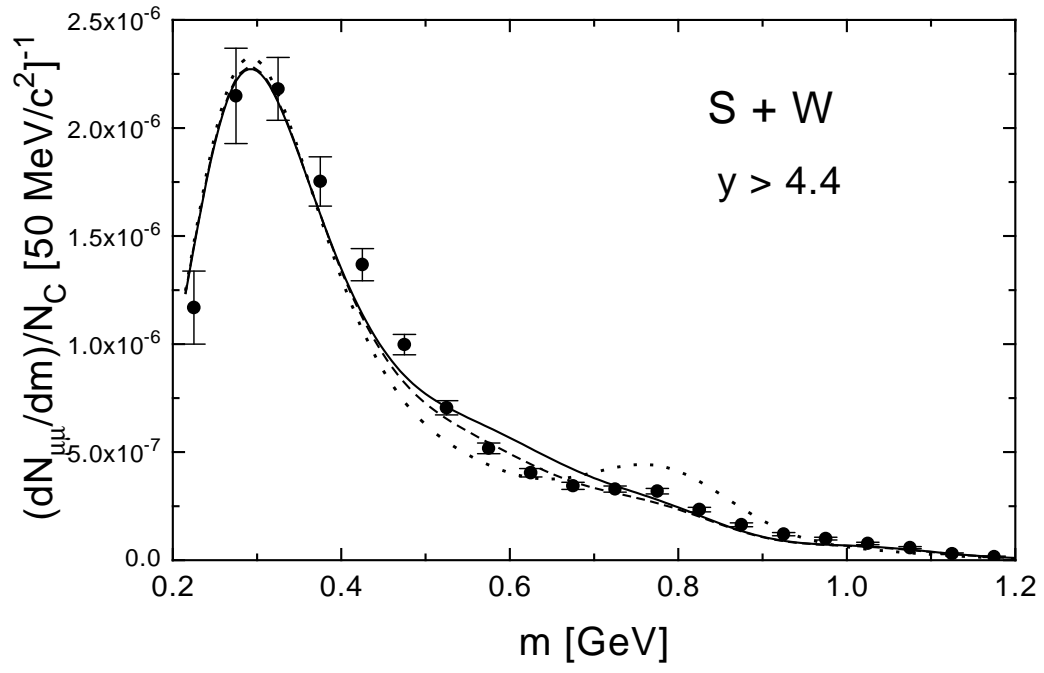


Figure 5b